An Overview of Integral Quadratic Constraints for Delayed Nonlinear and Parameter-Varying Systems

Harald Pfifer and Peter Seiler

Abstract—A general framework is presented for analyzing the stability and performance of nonlinear and linear parameter varying (LPV) time delayed systems. First, the input/output behavior of the time delay operator is bounded in the frequency domain by integral quadratic constraints (IQCs). A constant delay is a linear, time-invariant system and this leads to a simple, intuitive interpretation for these frequency domain constraints. This simple interpretation is used to derive new IQCs for both constant and varying delays. Second, the performance of nonlinear and LPV delayed systems is bounded using dissipation inequalities that incorporate IQCs. This step makes use of recent results that show, under mild technical conditions, that an IQC has an equivalent representation as a finite-horizon time-domain constraint. Numerical examples are provided to demonstrate the effectiveness of the method for both class of systems.

I. Introduction

This paper presents a framework to analyze nonlinear or linear parameter varying (LPV) time-delayed systems. In this framework the system is separated into a nonlinear or LPV system in feedback with a time delay. Stability and performance is considered for both constant and varying delays. The analysis uses the concept of integral quadratic constraints (IQCs) [26]. Specifically, IQCs describe the behavior of a system in the frequency domain in terms of an integral constraint on the Fourier transforms of the input/output signals. Several IQCs valid for constant and varying delays have already appeared in the literature, see e.g. [26], [18], [19].

This paper has two main contributions. The first contribution is to provide a simple interpretation for IQCs used to describe constant time delays. In particular, constant time delays are linear, time-invariant (LTI) systems and hence they have an equivalent frequency response representation. Thus IQCs valid for constant delays can, in most cases, be interpreted as a frequency dependent circle in the Nyquist plane. It is noted that this interpretation previously appeared in the robust control literature: "G"-scales for robustness analysis with real parameter uncertainty can be interpreted with circles in the complex plane [7], [9]. Here, the geometric interpretation is used to construct a new IQC valid for constant delays. Moreover, the frequency domain intepretation provides insight for generating a new IQC valid for time-varying delays even though such varying delays are not LTI. All these results are contained in Section IV.

The second contribution of this paper is to apply general IQCs for analysis of nonlinear and LPV delayed systems. The standard IQC stability theorem in [26] was formulated

with frequency domain conditions and hence requires the "nominal" part of the feedback interconnection to be an LTI system. An application of this stability theorem to LTI systems in feedback with a constant delay is given in [13]. Previous work on delayed nonlinear systems bounded the nonlinear elements of the system and the time delays by IQCs and considered this frequency domain approach to analyze a "nominal" LTI systems under IQCs, see e.g. [34]. Here, dissipation inequality conditions are derived to assess the stability and performance of "nominal" nonlinear and LPV systems in feedback with a delay. The dissipation inequalities are time-domain conditions but IQCs are typically expressed as frequency domain constraints. Thus the key technical issue is that the analysis approach requires an equivalent time-domain interpretation for an IQC. Previous work along these lines for constant IQCs has appeared in Chapter 8 of [16]. In fact, a large class of IQCs, under mild technical conditions, have an equivalent expression as a finite-horizon, time-domain integral as recently shown in [24], [40]. This time-domain expression enables IQCs to be easily incorporated into a dissipation inequality condition as shown in Section V. These analysis conditions can be formulated and efficiently solved as sum-of-squares optimizations [32] and semidefinite programs [4] for nonlinear and LPV delayed systems, respectively. Numerical examples for both system types are given in Section VI. These results complement recent robust performance conditions for LPV systems [38], [21], [36]. This paper builds upon [35]. In addition to the results in [35], it includes a detailed description of the generation of IQC multipliers for time delays.

There is a large body of literature on time-delayed systems as summarized in [16], [5]. The most closely related work is that contained in [13], [26], [18], [19] which use IQCs to derive stability conditions for LTI systems with constant or varying delays. As noted above, the contribution of this paper is to extend these results to nonlinear and LPV delayed systems. Lyapunov theory is an alternative framework in the literature of time-delayed systems [16], [15], [12]. This approach essentially constructs Lyapunov-Krasovskii or Lyapunov-Razumikhin functionals to assess the convergence of the free (initial-condition) response of the delayed system. Stability conditions for nonlinear [30], [31] and LPV [44] delayed systems have been developed in the Lyapunov framework. These methods treat the time delay as integrated with the dynamics of the plant. This is in contrast to the approach considered here which uses input-output stability (forced response) and separates the time delay from the "nominal" plant dynamics. A benefit of the IQC framework is that extends naturally to systems with many delays and/or uncertainties. On the other hand, some stability conditions

H. Pfifer and P. Seiler are with the Aerospace Engineering and Mechanics Department, University of Minnesota, emails: `hpfifer@umn.edu`, `seiler@aem.umn.edu`

in the Lyapunov-Krasovskii framework appear to use time-varying quadratic constraints that do not have counterparts in the IQC literature. This connection is not pursued here but may lead to new insights within the IQC framework.

II. NOTATION

$\mathbb{R}$ and $\mathbb{C}$ denote the set of real and complex numbers, respectively. $\mathbb{RL}_\infty$ denotes the set of rational functions with real coefficients that are proper and have no poles on the imaginary axis. $\mathbb{RH}_\infty$ is the subset of functions in $\mathbb{RL}_\infty$ that are analytic in the closed right half of the complex plane. $\mathbb{C}^{m \times n}$, $\mathbb{RL}_\infty^{m \times n}$ and $\mathbb{RH}_\infty^{m \times n}$ denote the sets of $m \times n$ matrices whose elements are in $\mathbb{R}$, $\mathbb{C}$, $\mathbb{RL}_\infty$, $\mathbb{RH}_\infty$, respectively. A single superscript index is used for vectors, e.g. $\mathbb{R}^n$ denotes the set of $n \times 1$ vectors whose elements are in $\mathbb{R}$. For $z \in \mathbb{C}$, $\bar{z}$ denotes the complex conjugate of z. For a matrix $M \in \mathbb{C}^{m \times n}$, M^T denotes the transpose and M^* denotes the complex conjugate transpose. The para-Hermitian conjugate of $G \in \mathbb{RL}_\infty^{m \times n}$, denoted as $G^\sim$, is defined by $G^\sim(s) := G(-\bar{s})^*$. Note that on the imaginary axis, $G^\sim(j\omega) = G(j\omega)^*$. $L_2^n[0, \infty)$ is the space of functions $v : [0, \infty) \to \mathbb{R}^n$ satisfying $\|v\| < \infty$ where

$$\|v\| := \left[\int_0^\infty v(t)^T v(t) \, dt \right]^{0.5} \tag{1}$$

Given $v \in L_2^n[0, \infty)$, v_T denotes the truncated function:

$$v_T(t) := \begin{cases} v(t) & \text{for } t \leq T \\ 0 & \text{for } t > T \end{cases} \tag{2}$$

The extended space, denoted L_{2e}, is the set of functions v such that $v_T \in L_2$ for all $T \geq 0$. Finally, the Fourier Transform $\hat{v} := \mathcal{F}(v)$ maps the time domain signal $v \in L_2^n[0, \infty)$ to the frequency domain by

$$\hat{v}(j\omega) := \int_0^\infty e^{-j\omega t} v(t) dt \tag{3}$$

III. PROBLEM FORMULATION

Consider the time-delay system given by the feedback interconnection of a nonlinear, time-invariant system $\tilde{G}$ and a (constant) delay $\mathcal{D}_\tau$ as shown in Fig. 1. The delay $\tilde{w} = \mathcal{D}_\tau(v)$ is defined by $\tilde{w}(t) = v(t - \tau)$ where τ specifies the delay. The input/output signals can, in general, be vector-valued with $\tilde{w}(t), v(t) \in \mathbb{R}^{n_v}$. The remaining signals in the interconnection have dimensions $d(t) \in \mathbb{R}^{n_d}$ and $e(t) \in \mathbb{R}^{n_e}$. The feedback interconnection is obtained by closing the upper channels of $\tilde{G}$ with the time delay $\mathcal{D}_\tau$. This feedback interconnection, denoted as $F_u(\tilde{G}, \mathcal{D}_\tau)$, gives a time-delay system with input d and output e.

A robust stability approach to analysis is pursued in this paper. Thus it will be more convenient to express the system in terms of the deviation between the delayed and the (nominal) undelayed signal, $\mathcal{S}_\tau(v) := \mathcal{D}_\tau(v) - v$. A loop transformation, shown in Fig. 2, can be used to express the feedback interconnection as $F_u(G, \mathcal{S}_\tau)$. This loop-shift amounts to the replacement $\tilde{w} = w + v$ where $w := \mathcal{S}_\tau(v)$. The system G
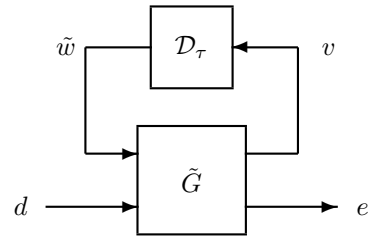

Fig. 1. Feedback interconnection with time delay $\mathcal{D}_\tau$

obtained after this loop-shift is assumed to be described by the following finite-dimensional differential equation:

$$\begin{aligned} \dot{x}_G &= f(x_G, w, d) \\ v &= h_1(x_G, w, d) \\ e &= h_2(x_G, w, d) \end{aligned} \tag{4}$$

where $x_G(t) \in \mathbb{R}^{n_G}$ is the state of G at time t.
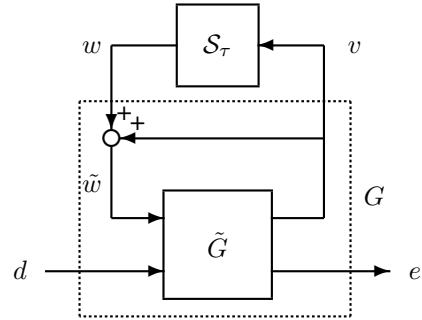

Fig. 2. Loop transformation to $F_u(G, \mathcal{S}_\tau)$

An input-output approach is used in this paper to analyze the stability and performance of the time-delay system. For a given delay τ, the induced L_2 gain for the feedback interconnection from d to e is defined as:

$$\|F_u(G, \mathcal{S}_\tau)\| := \sup_{0 \neq d \in L_2^{n_d}[0, \infty), \ x_G(0) = 0} \frac{\|e\|}{\|d\|} \tag{5}$$

It is important to note that the restriction to time $t \geq 0$ implicitly assumes zero initial conditions for both $\mathcal{D}_\tau$ and $\mathcal{S}_\tau$. Specifically, $\tilde{w} = \mathcal{D}_\tau(v)$ is more precisely defined on $L_2[0, \infty)$ by $\tilde{w}(t) = 0$ for $t \in [0, \tau)$ and $\tilde{w}(t) = v(t - \tau)$ for $t \geq \tau$. Similarly, $w = \mathcal{S}_\tau(v)$ is defined on $L_2[0, \infty)$ by $w(t) = -v(t)$ for $t \in [0, \tau)$ and $w(t) = v(t - \tau) - v(t)$ for $t \geq \tau$. The notion of finite gain stability used in this paper is defined next.

Definition 1. The feedback interconnection of G and $\mathcal{S}_\tau$ is stable if the interconnection is well-posed and if the mapping from d to e has finite L_2 gain, i.e. there exists a finite constant $\gamma > 0$ such that $\|F_u(G, \mathcal{S}_\tau)\| \leq \gamma$.

Two main analysis problems are considered. First, determine the largest value of $\bar{\tau}$ such that the feedback interconnection is stable for all $\tau \in [0, \bar{\tau}]$. The first problem gives the *delay margin* for the system. Second, given a delay τ less than the delay margin, determine the largest induced L_2 gain from d

to e. The second problem gives the performance of the system for a fixed level of delay as measured by the L_2 gain.

Since the delay is constant, $\mathcal{D}_\tau$ defines a linear, time-invariant (LTI) system. In this case the delay has a well-known frequency domain representation. For constant delays $w = \mathcal{D}_\tau(v)$ can be expressed in the frequency domain as $\hat{w}(j\omega) = \hat{\mathcal{D}}_\tau(j\omega)\hat{v}(j\omega)$ where $\hat{\mathcal{D}}_\tau(j\omega) := e^{-j\omega\tau}$. In other words, the delay is equivalent to a frequency-by-frequency multiplication by $\hat{\mathcal{D}}_\tau$. Similarly, $\mathcal{S}_\tau$ has the frequency response $\hat{\mathcal{S}}_\tau(j\omega) = e^{-j\omega\tau} - 1$. These frequency domain relations are used in the next section to derive simple, geometric constraints satisfied by the input/output signals of $\mathcal{S}_\tau$. Additional technical details on the frequency domain can be found in standard textbooks, e.g. [8].

Up to this point the presentation has focused entirely on constant delays. However, the analysis problems can be extended to consider time-varying delays. The time-varying delay $\tilde{w} = \mathcal{D}_{\bar{\tau},r}(v)$ is defined by $\tilde{w}(t) = v(t-\tau(t))$ where $\tau(t)$ specifies the delay at time t. The subscripts $\bar{\tau}$ and r denote that the delay satisfies $\tau(t) \in [0, \bar{\tau}]$ and $|\dot{\tau}(t)| \le r$ for all $t \ge 0$. In other words, $\bar{\tau}$ is the maximum delay and r bounds the rate of variation. If $r = 0$ then $\mathcal{D}_{\bar{\tau},r}$ corresponds to a constant delay with value $\tau \in [0, \bar{\tau}]$. In addition, define $w = \mathcal{S}_{\bar{\tau},r}(v)$ by $w = \mathcal{D}_{\bar{\tau},r}(v) - v$, i.e. $\mathcal{S}_{\bar{\tau},r}$ is the deviation from the nominal undelayed signal. A time-varying delay is not a time-invariant system. Hence it does not have a valid frequency-response interpretation. However, the frequency-domain intuition can be used to derive constraints on the input/output signals of a time-varying delay (Section IV-C).

IV. FREQUENCY DOMAIN INEQUALITIES

This section describes different frequency domain constraints on the delay operator that can be incorporated into the input/output analysis. The basic idea builds on common frequency domain inequalities that have appeared in the literature, e.g. [41], [26], [16]. Given a constant delay τ, define the LTI system ϕ as:

$$\phi(s) := 2\frac{(s\tau)^2 + 3.5s\tau + 10^{-6}}{(s\tau)^2 + 4.5s\tau + 7.1}. \tag{6}$$

Fig. 3(a) shows the Bode magnitude plots for $\hat{\mathcal{S}}_\tau$ (solid line) and ϕ (dashed line) The weight ϕ is chosen to satisfy $|\hat{\mathcal{S}}_\tau(j\omega)| \le |\phi(j\omega)|$ for all ω and hence $\hat{\mathcal{S}}_\tau$ is a member of the following frequency weighted uncertainty set:
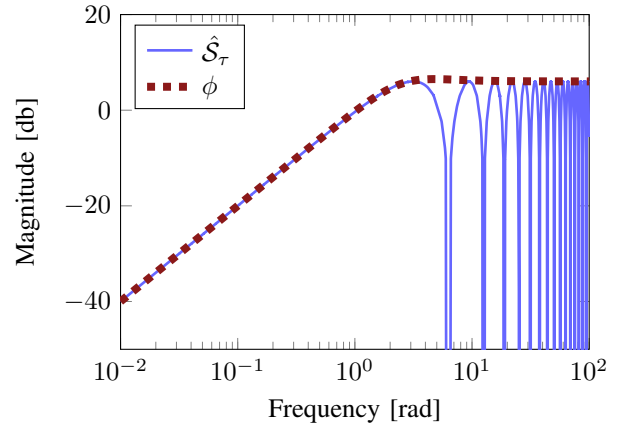
$$\{\Delta : |\Delta(j\omega)| \le |\phi(j\omega)| \ \forall \omega\} \tag{7}$$

This magnitude bound has simple geometric and algebraic interpretations at each frequency. The geometric interpretation of this uncertainty set is a circle in the complex Nyquist plane as depicted in Fig. 3(b). $\hat{\mathcal{S}}_\tau(j\omega)$ follows a circle centered at -1 with radius 1 (dashed circle). At each frequency $\hat{\mathcal{S}}_\tau(j\omega)$ lies within the shaded circle of radius $|\phi(j\omega)|$ centered at the origin. An algebraic interpretation can be given in terms of a quadratic constraint. The Fourier transforms for any
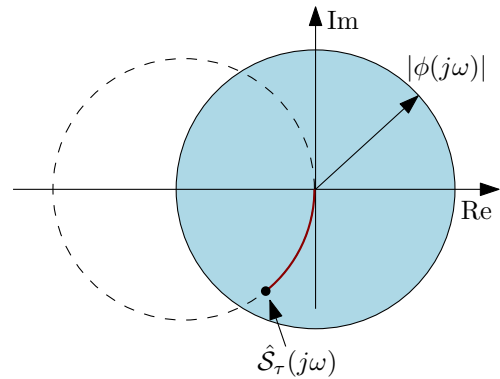
input/output pair $w = \mathcal{S}_\tau(v)$ must satisfy the following quadratic inequality at each frequency:

$$\begin{bmatrix} \hat{v}(j\omega) \\ \hat{w}(j\omega) \end{bmatrix}^* \begin{bmatrix} |\phi(j\omega)|^2 & 0 \\ 0 & -1 \end{bmatrix} \begin{bmatrix} \hat{v}(j\omega) \\ \hat{w}(j\omega) \end{bmatrix} \ge 0 \tag{8}$$

This quadratic constraint is just a restatement of the norm bound on $\hat{\mathcal{S}}_\tau$ at each frequency. Using this basic intuition, additional geometric constraints in the Nyquist plane can be expressed in the form of quadratic constraints at each frequency. Pointwise quadratic constraints are discussed further in Section IV-A for general LTI systems and the application to constant time delays is given in Section IV-B.

(a) Bode Magnitude Plot for $\hat{\mathcal{S}}_\tau$ and bound ϕ

(b) Circle Interpretation for $|\hat{\mathcal{S}}_\tau(j\omega)| \le |\phi(j\omega)|$

Fig. 3. Norm Bound on $\hat{\mathcal{S}}_\tau$

A. Pointwise Quadratic Constraints

This section describes pointwise quadratic constraints for an LTI system Δ. For simplicity assume Δ is a single input, single output (SISO) system. The input/output relation $w = \Delta v$ is represented in the frequency domain by $\hat{w}(j\omega) = \hat{\Delta}(j\omega)\hat{v}(j\omega)$. This representation can be used to bound the input/output signals using frequency-by-frequency quadratic constraints (QC).

Definition 2. Let $\Pi : j\mathbb{R} \to \mathbb{C}^{2\times 2}$ be a Hermitian-valued function, called a "multiplier". Two signals $v, w \in L_2[0,\infty)$ satisfy the QC defined by Π if the following inequality holds

$$\begin{bmatrix} \hat{v}(j\omega) \\ \hat{w}(j\omega) \end{bmatrix}^* \Pi(j\omega) \begin{bmatrix} \hat{v}(j\omega) \\ \hat{w}(j\omega) \end{bmatrix} \geq 0, \ \forall \omega \quad (9)$$

Moreover, the LTI system Δ satisfies the QC defined by Π, denoted $\Delta \in \mathrm{QC}(\Pi)$, if (9) holds for all $v \in L_2[0,\infty)$ and $w = \Delta v$.

These QCs have an intuitive geometric interpretation. Specifically, the QCs can be interpreted as circle or half-plane constraints on the Nyquist plot of $\hat{\Delta}(j\omega)$. Partition the 2×2 multiplier as $\Pi = \begin{bmatrix} \pi_{11} & \pi_{21}^* \\ \pi_{21} & \pi_{22} \end{bmatrix}$. The diagonal entries are real since Π is Hermitian. In addition, the QC is unaffected by positive scaling. Specifically, let $\lambda : j\mathbb{R} \to \mathbb{R}$ be a frequency dependent scaling that satisfies $\lambda(j\omega) > 0 \ \forall \omega$. Then $\Delta \in \mathrm{QC}(\Pi)$ if and only if $\Delta \in \mathrm{QC}(\lambda\Pi)$. Thus, without loss of generality, the multiplier can be normalized to have $\pi_{22}(j\omega) = -1, 0,$ or $+1$ for all ω. This normalization provides a clearer geometric interpretation for the QC as described in the next lemma.

Lemma 1. Let Δ be an LTI system satisfying $\Delta \in \mathrm{QC}(\Pi)$. At each frequency the QC can be normalized to one of three cases:

1) If $\pi_{22}(j\omega) = -1$ then
$$|\hat{\Delta}(j\omega) - \pi_{21}(j\omega)| \leq \sqrt{\pi_{11}(j\omega) + |\pi_{21}(j\omega)|^2} \quad (10)$$

2) If $\pi_{22}(j\omega) = 0$ then
$$0 \leq \pi_{11}(j\omega) + \hat{\Delta}(j\omega)^* \pi_{21}(j\omega) + \pi_{21}(j\omega)\hat{\Delta}(j\omega) \quad (11)$$

3) If $\pi_{22}(j\omega) = +1$ then
$$|\hat{\Delta}(j\omega) - \pi_{21}(j\omega)| \geq \sqrt{\pi_{11}(j\omega) + |\pi_{21}(j\omega)|^2} \quad (12)$$

Proof. The QC in Equation 9 must hold for all input signals $v \in L_2[0,\infty)$. Since $\hat{w}(j\omega) = \hat{\Delta}(j\omega)\hat{v}(j\omega)$, the QC can be rewritten as (dropping the dependence on $j\omega$):

$$0 \leq \begin{bmatrix} 1 \\ \hat{\Delta} \end{bmatrix}^* \Pi \begin{bmatrix} 1 \\ \hat{\Delta} \end{bmatrix} = \pi_{11} + \hat{\Delta}^* \pi_{21} + \pi_{21}^* \hat{\Delta} - \hat{\Delta}^* \pi_{22} \hat{\Delta} \quad (13)$$

If $\pi_{22}(j\omega) = 0$ then this simplifies to Equation 11. If $\pi_{22}(j\omega) = \pm 1$ then complete the square to express Equation 13 as in Equation 10 or Equation 12. $\qquad \square$

Equation 10 defines a circle and its interior (a disk) in the complex plane centered at $\pi_{21}(j\omega)$ with radius given by $\sqrt{\pi_{11}(j\omega) + |\pi_{21}(j\omega)|^2}$. Equation 11 defines a half plane in the complex plane. For example if $\pi_{21}(j\omega) = 1$ then (11) defines the half plane given by $\mathrm{Re}(\hat{\Delta}(j\omega)) \geq -\frac{1}{2}\pi_{11}(j\omega)$. Finally, the case where $\pi_{22}(j\omega) = +1$ corresponds to the non-convex set described by a circle and its exterior. Thus a QC defines a circle or half-plane constraint in the complex (Nyquist) plane at each frequency. The dissipation theory developed below is only valid for $\pi_{22}(j\omega) < 0$ and hence the focus will be on quadratic constraints that are described by disks. "G"-scales used for robustness analysis with real

parameter uncertainty can also be interpreted as a circle constraint [7], [9].

Multiple QCs can be combined to obtain new QCs. If the LTI system Δ satisfies the QCs defined by $\{\Pi_k\}_{k=1}^N$ then Δ also satisfies the QC defined by $\Pi(\lambda) := \sum_{k=1}^N \lambda_k \Pi_k$ for any real, non-negative numbers $\{\lambda_k\}_{k=1}^N$. $\Pi(\lambda)$ is called a conic combination of the multipliers $\{\Pi_k\}_{k=1}^N$. This fact enables many QCs on Δ to be incorporated into an analysis. However, it is important to recognize that such conic combinations have certain limitations. The main limitation is that any conic combination is, by Lemma 1, just a circle or half-plane constraint in the complex plane. As a concrete example, consider the circle constraint on $\mathcal{S}_\tau$ described by Equation 8 and shown in Fig. 3(b). The corresponding multiplier is $\Pi_1(j\omega) := \begin{bmatrix} |\phi(j\omega)|^2 & 0 \\ 0 & -1 \end{bmatrix}$. $\mathcal{S}_\tau$ also satisfies the QC defined by $\Pi_2 = \begin{bmatrix} 0 & -1 \\ -1 & -1 \end{bmatrix}$. This second multiplier corresponds to a circle centered at -1 with unit radius, shown as the dashed circle in Fig. 3(b). Thus $\mathcal{S}_\tau$ lies in the intersection of the shaded circle centered at the origin (defined by Π_1) and the dashed circle centered at -1 (defined by Π_2). However, the conic combinations $\Pi(\lambda) := \lambda_1 \Pi_1 + \lambda_2 \Pi_2$ correspond to circles that "cover", i.e. outer bound, this intersection.

Remark. In fact, conic combinations of two QC multipliers are "tight". Roughly, the conic combinations $\lambda_1 \Pi_1 + \lambda_2 \Pi_2$ define the smallest regions that contain the intersection of the sets defined by Π_1 and Π_2. This statement is a geometric consequence of the S-procedure lossless theorem for complex constraints [10], [8], [17]. However the S-procedure is not lossless, in general, for three or more QCs. Hence conic combinations need not provide a tight bound on the set described by the intersection of three or more multipliers.

The QCs defined above for SISO systems can be extended, with only notational changes, to multiple-input, multiple output (MIMO) systems. It will be sufficiently general for the time-delay analysis to consider repeated systems. Let Δ be a SISO, LTI system and define the $n \times n$ repeated system $w = (\Delta \cdot I_n)(v)$ by $w_i = \Delta v_i$ for $i = 1, \ldots, n$. If $\Delta \in \mathrm{QC}(\Pi)$ for a 2×2 multiplier Π then the following QC holds for all $v \in L_2^n[0,\infty)$ and $w = (\Delta \cdot I_n)v$:

$$\begin{bmatrix} \hat{v}(j\omega) \\ \hat{w}(j\omega) \end{bmatrix}^* \begin{bmatrix} \pi_{11}(j\omega) \cdot I_n & \pi_{12}(j\omega) \cdot I_n \\ \pi_{21}(j\omega) \cdot I_n & \pi_{22}(j\omega) \cdot I_n \end{bmatrix} \begin{bmatrix} \hat{v}(j\omega) \\ \hat{w}(j\omega) \end{bmatrix} \geq 0, \ \forall \omega \quad (14)$$

Moreover Δ is LTI and hence $\Delta \cdot I_n$ commutes with any $n \times n$, frequency-dependent matrix D, i.e. $D(\Delta \cdot I_n) = (\Delta \cdot I_n)D$. Thus the frequency-scaled system $\bar{\Delta} := D\Delta D^{-1}$ also satisfies the QC in Equation 14. Let $(\bar{v}, \bar{w})$ be any input-output pair for the scaled system $\bar{\Delta}$ as shown in Fig. 4. The associated input/output pair for the original system $w = (\Delta \cdot I_n)v$ is related to the input/output pair for the scaled system by $\bar{w} = Dw$ and $\bar{v} = Dv$. Hence, $\Delta \cdot I_n$ also satisfies the QC with any multiplier $\Pi_n : j\mathbb{R} \to \mathbb{C}^{2n \times 2n}$ of the form

$$\Pi_n(j\omega) := \begin{bmatrix} \pi_{11}(j\omega) \cdot X(j\omega) & \pi_{12}(j\omega) \cdot X(j\omega) \\ \pi_{21}(j\omega) \cdot X(j\omega) & \pi_{22}(j\omega) \cdot X(j\omega) \end{bmatrix} \quad (15)$$

where $X(j\omega) := D(j\omega)^*D(j\omega) \geq 0$. This more general, frequency-scaled multiplier can be used to reduce the conservatism in the analysis. The use of X is analogous to the multipliers used in classical robustness analysis, e.g. the structured singular value μ [37], [6], [29], [45].
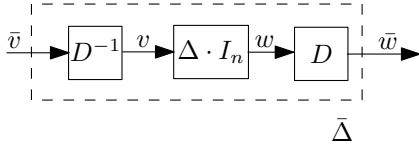

Fig. 4. Scaling of the Operator $\Delta \cdot I_n$

B. Application to Constant Time Delays

There are numerous circle constraints that can be used to bound $\mathcal{S}_\tau$. A few examples are provided below to illustrate how the frequency-domain geometric interpretation can be used to impose constraints on $\mathcal{S}_\tau$. The QCs on $\mathcal{S}_\tau$ can be converted, if needed, into equivalent QCs on $\mathcal{D}_\tau$ by reversing the loop-transformation, i.e. by replacing $w = \tilde{w} - v$ in the QC. For clarity, the QC multipliers are given assuming $\mathcal{S}_\tau$ is SISO. However, as described previously, frequency-dependent (matrix) scalings can be introduced if $\mathcal{S}_\tau$ is MIMO.

Example 1. The Nyquist plot for $\hat{\mathcal{S}}_\tau$ follows a circle centered at -1 with radius 1. Hence, the most basic QC to bound $\mathcal{S}_\tau$ describes exactly this circle. This corresponds to the following multiplier:

$$\Pi_1 := \begin{bmatrix} 0 & -1 \\ -1 & -1 \end{bmatrix}. \tag{16}$$

Example 2. The multiplier in Example 1 does not depend on the value of the time delay τ. Thus the multiplier in (16) describes a very conservative constraint due to this delay independence. A simple delay dependent constraint is obtained from the frequency response $\hat{\mathcal{S}}_\tau(j\omega) = e^{-j\omega\tau} - 1$. Thus at each frequency $\hat{\mathcal{S}}_\tau(j\omega)$ lies within a circle centered at the origin of radius $|\hat{\mathcal{S}}_\tau(j\omega)|$. The multiplier Π_2 for this circle is given by:

$$\Pi_2(j\omega) := \begin{bmatrix} \left|\hat{\mathcal{S}}_\tau(j\omega)\right|^2 & 0 \\ 0 & -1 \end{bmatrix} \tag{17}$$

Example 3. A smaller circle constraint can be constructed for $\mathcal{S}_\tau$. The midpoint of the segment connecting $\hat{\mathcal{S}}_\tau(j\omega)$ and the origin is given by $\frac{1}{2}\hat{\mathcal{S}}_\tau(j\omega)$. The following multiplier Π_3 defines a circle centered at this midpoint with radius equal to the absolute value of this midpoint.

$$\Pi_3(j\omega) := \begin{bmatrix} 0 & \frac{1}{2}\hat{\mathcal{S}}_\tau(j\omega) \\ \frac{1}{2}\hat{\mathcal{S}}_\tau(j\omega) & -1 \end{bmatrix} \tag{18}$$

The QC described by Π_3 is shown in Fig. 5.

As can be seen by the examples, there exist numerous ways to bound $\mathcal{S}_\tau$ using a QC. More examples are given in literature.
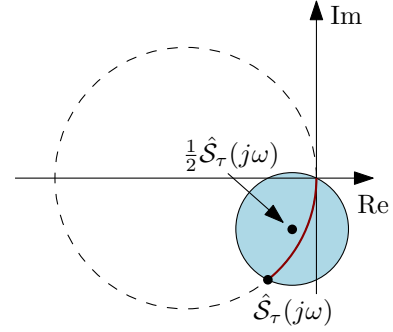

Fig. 5. "Small" Circle Constraint on $\mathcal{S}_\tau$ described by QC(Π_3)

For instance, in [26] a multiplier is provided that corresponds to a circle whose center moves along the imaginary axis with frequency. Unfortunately there are no general rules for which specific QC will provide the most useful stability and performance analysis results. It might seem intuitive to use the QC that describes the smallest area circle. However, this does not, in general, provide the least conservative analysis results. The best solution is to specify many different QCs and allow a numerical algorithm select the best conic combination. This will be described further in the next section.

Two practical issues must be addressed to make these QCs useful for numerical analysis. First, recall that a system $F_u(G, \mathcal{S}_\tau)$ has delay margin of $\bar{\tau}$ if it is stable for all delays $\tau \in [0, \bar{\tau}]$. Thus the delay margin analysis requires a QC that covers $\mathcal{S}_\tau$ for all $\tau \in [0, \bar{\tau}]$. For example, the following multiplier covers $\mathcal{S}_\tau$ for all constant delays $\tau \in [0, \bar{\tau}]$:

$$\tilde{\Pi}_2(j\omega) := \begin{cases} \begin{bmatrix} \left|\hat{\mathcal{S}}_{\bar{\tau}}(j\omega)\right|^2 & 0 \\ 0 & -1 \end{bmatrix} & \text{if } \omega \leq \frac{\pi}{\bar{\tau}} \\ \begin{bmatrix} 4 & 0 \\ 0 & -1 \end{bmatrix} & \text{else} \end{cases} \tag{19}$$

At each low frequency ($\omega \leq \frac{\pi}{\bar{\tau}}$), $\tilde{\Pi}_2$ describes a circle centered at the origin that covers all Nyquist curves $\hat{\mathcal{S}}_\tau(j\omega)$ for $\tau \in [0, \bar{\tau}]$. This is essentially equivalent to the multiplier in Example 2 at low frequencies. However, these circles fail to have the desired covering property at higher frequencies. For $\omega > \frac{\pi}{\bar{\tau}}$, the multiplier $\tilde{\Pi}_2$ is set equal to a circle centered at the origin of radius 2. This ensures that the QC defined by $\tilde{\Pi}_2$ covers the entire Nyquist curve of $\hat{\mathcal{S}}_\tau$ at high frequencies. The other QC multipliers specified in the examples can be similarly modified at high frequencies for use in delay margin analysis.

The second practical issue is the need to approximate a QC multiplier with a rational function so that state-space numerical methods can be applied. For example $\tilde{\Pi}_2$ is a non-rational multiplier that describes a circle at each frequency. Let $\phi_2(s)$ be any stable LTI system that satisfies $|\phi_2(j\omega)| \geq |\hat{\mathcal{S}}_{\bar{\tau}}(j\omega)|$ for $\omega \leq \frac{\pi}{\bar{\tau}}$ and $|\phi_2(j\omega)| \geq 2$ for $\omega > \frac{\pi}{\bar{\tau}}$. The specific choice in Equation 6 satisfies these constraints. Then $\mathcal{S}_{\bar{\tau}}$ satisfies the QC

defined by the following (rational) multiplier for all $\tau \in [0, \bar{\tau}]$:

$$\bar{\Pi}_2(j\omega) = \begin{bmatrix} |\phi_2(j\omega)|^2 & 0 \\ 0 & -1 \end{bmatrix} \quad (20)$$

$\bar{\Pi}_2(j\omega)$ describes a circle with larger radius than $\tilde{\Pi}_2(j\omega)$ due to the choice of $\phi_2(s)$. Hence $\mathcal{S}_\tau \in \mathrm{QC}(\tilde{\Pi}_2) \subset \mathrm{QC}(\bar{\Pi}_2)$ for all $\tau \in [0, \bar{\tau}]$. $\bar{\Pi}_2$ is the weighted multiplier (Equation 8) discussed earlier in the section. It is commonly used in the literature to analyze time delayed systems [41], [26], [16].

Remark. Numerical tools can be used to aid the construction of rational function approximations for more complicated multipliers. Briefly consider a (non-rational) multiplier $\Pi = \begin{bmatrix} \pi_{11} & \pi_{21}^* \\ \pi_{21} & -1 \end{bmatrix}$. By Lemma 1 the QC associated with this multiplier defines a circle centered at $\pi_{21}(j\omega)$ with radius given by $\sqrt{\pi_{11}(j\omega) + |\pi_{21}(j\omega)|^2}$. A rational approximation $\bar{\Pi}$ can be computed by the following procedure. Fit π_{21} with a rational approximation $\bar{\pi}_{21}$, e.g. using the Matlab function `fitfrd` or some other numerical optimization. This approximation will introduce some fitting error and hence the radius of the rational multiplier may need to be increased to ensure $\mathcal{S}_\tau$ is covered. This would require $\bar{\pi}_{11}$ to satisfy a lower bound constraint on its magnitude. A rational approximation with a lower bound magnitude constraint can be computed for $\bar{\pi}_{11}$, e.g. using the Matlab function `fitmagfrd`. Using this procedure, the following rational fit was constructed for Π_3 that covers $\mathcal{S}_\tau$ for all delays $\tau \in [0, \bar{\tau}]$

$$\bar{\Pi}_3(j\omega) := \begin{bmatrix} 0 & \phi_3^*(j\omega) \\ \phi_3(j\omega) & -1 \end{bmatrix} \quad (21)$$

where

$$\phi_3(j\omega) := \frac{-2.19\left(\frac{j\omega}{\bar{\tau}}\right)^2 + 9.02\left(\frac{j\omega}{\bar{\tau}}\right) + 0.089}{\left(\frac{j\omega}{\bar{\tau}}\right)^2 - 5.64\left(\frac{j\omega}{\bar{\tau}}\right) - 17.0}. \quad (22)$$

Note that π_{21} does not need to be stable, as is the case with the given choice of ϕ_3.

C. Application to Varying Time Delays

The QCs given for constant time delays hold at each frequency. These point-wise QCs fall within a more general framework based on integral quadratic constraints (IQCs) introduced in [26]. A definition is now given for IQCs that extends the one given in Definition 2 for QCs.

Definition 3. Let $\Pi : j\mathbb{R} \rightarrow \mathbb{C}^{(m_1+m_2)\times(m_1+m_2)}$ be a Hermitian-valued function. Two signals $v \in L_2^{m_1}[0, \infty)$ and $w \in L_2^{m_2}[0, \infty)$ satisfy the integral quadratic constraint (IQC) defined by Π if

$$\int_{-\infty}^{\infty} \begin{bmatrix} \hat{v}(j\omega) \\ \hat{w}(j\omega) \end{bmatrix}^* \Pi(j\omega) \begin{bmatrix} \hat{v}(j\omega) \\ \hat{w}(j\omega) \end{bmatrix} d\omega \geq 0 \quad (23)$$

where $\hat{v}(j\omega)$ and $\hat{w}(j\omega)$ are Fourier transforms of v and w, respectively. A bounded, causal operator $\Delta : L_{2e}^{m_1}[0, \infty) \rightarrow L_{2e}^{m_2}[0, \infty)$ satisfies the IQC defined by Π, denoted $\Delta \in \mathrm{IQC}(\Pi)$, if (23) holds for all $v \in L_2^{m_1}[0, \infty)$ and $w = \Delta(v)$.

Clearly, if the QC holds pointwise in frequency it also holds when integrated over all frequencies, i.e. $\Delta \in \mathrm{QC}(\Pi)$ implies $\Delta \in \mathrm{IQC}(\Pi)$. The converse is not true and the more general IQC theory can be applied to nonlinear and/or time varying perturbations. IQCs were introduced in [26] to provide a general framework for robustness analysis. Here, the focus will be on the use of IQCs to describe the input/output behavior of time-varying delays. A time-varying delay is not a time-invariant system. Hence the point-wise QCs cannot be used and the more general IQCs are required. However, the frequency domain arguments used to construct QCs for constant delays can provide intuition regarding IQCs for time-varying delays. The remainder of this section reviews known IQCs for time-varying delays [18], [19], [16]. In addition a new IQC for time-varying delays is constructed using the frequency domain intuition gained from constant-delays.

Recall the notation $\mathcal{D}_{\bar{\tau},r}$ and $\mathcal{S}_{\bar{\tau},r}$ introduced for varying delays where $\bar{\tau}$ and r are bounds on the maximum delay and rate of variation, respectively. The basic IQCs for time-varying delays arise from two simple norm bounds. First, if $r < 1$ then the induced L_2 gain of the varying-time delay can be bounded by $\|\mathcal{D}_{\bar{\tau},r}\| \leq \frac{1}{\sqrt{1-r}}$ (Section 3.2 in [16] and Lemma 1 in [19]). Second, let $\mathcal{S}_{\bar{\tau},r} \circ \frac{1}{s}$ denote $\mathcal{S}_{\bar{\tau},r}$ composed with an integrator at the input. The induced L_2 gain of this combined system can be bounded by $\|\mathcal{S}_{\bar{\tau},r} \circ \frac{1}{s}\| \leq \bar{\tau}$ (Lemma 1 in [18]). These two bounds are tight in the sense that the gain is achieved for some input signal v and time-varying delay $\tau(t)$ that satisfies the bounds $\bar{\tau}$ and r (Lemma 1 in [19]). Three IQCs are now provided for time-varying delays. These examples parallel the QCs provided in the previous subsection for constant delays. For clarity the multipliers are expressed assuming $\mathcal{D}_{\bar{\tau},r}$ and $\mathcal{S}_{\bar{\tau},r}$ are SISO. The extension to the MIMO case is discussed below.

Example 4. Let $\tilde{w} = \mathcal{D}_{\bar{\tau},r}(v)$ be a time-varying delay satisfying $r < 1$. The bound $\|\mathcal{D}_{\bar{\tau},r}\| \leq \frac{1}{\sqrt{1-r}}$ implies that $\|\tilde{w}\| \leq \frac{1}{\sqrt{1-r}}\|v\|$ for all input signals $v \in L_2[0, \infty)$. After performing the loop-transformation $w := \mathcal{S}_{\bar{\tau},r}(v)$, i.e. $\tilde{w} = w + v$, this inequality can be written as:

$$\int_0^{\infty} \begin{bmatrix} v(t) \\ w(t) \end{bmatrix}^T \begin{bmatrix} \frac{r}{1-r} & -1 \\ -1 & -1 \end{bmatrix} \begin{bmatrix} v(t) \\ w(t) \end{bmatrix} dt \geq 0 \quad (24)$$

By Parseval's theorem, this inequality can be equivalently expressed in the frequency domain as:

$$\int_{-\infty}^{\infty} \begin{bmatrix} \hat{v}(j\omega) \\ \hat{w}(j\omega) \end{bmatrix}^* \begin{bmatrix} \frac{r}{1-r} & -1 \\ -1 & -1 \end{bmatrix} \begin{bmatrix} \hat{v}(j\omega) \\ \hat{w}(j\omega) \end{bmatrix} d\omega \geq 0 \quad (25)$$

Thus $\mathcal{S}_{\bar{\tau},r}$ satisfies the IQC defined by the following multiplier:

$$\Pi_4 := \begin{bmatrix} \frac{r}{1-r} & -1 \\ -1 & -1 \end{bmatrix} \quad (26)$$

This multiplier is analogous to the multiplier Π_1 given in Example 1 for constant delays. Π_1 corresponds to a unit circle in the Nyquist plane centered at -1. At each frequency Π_4 can also be viewed as a circle centered at -1 but with radius enlarged to $\frac{1}{\sqrt{1-r}} > 1$ to account for the varying

delays. However this is not a precise statement since the constraints defined by IQC(Π_4) only hold when integrated over all frequencies.

Example 5. The multiplier in Example 4 depends on the rate of variation r but does not depend on the maximum delay $\bar{\tau}$. Proposition 2 in [19] gives a delay-dependent IQC that can be used to reduce the conservatism. The IQC in [19] depends on a rational bounded transfer function $\phi_5(s)$ that satisfies:

$$|\phi_5(j\omega)| > \begin{cases} \bar{\tau}|\omega| & \text{if } \bar{\tau}|\omega| \leq 1 + \frac{1}{\sqrt{1-r}} \\ 1 + \frac{1}{\sqrt{1-r}} & \text{if } \bar{\tau}|\omega| > 1 + \frac{1}{\sqrt{1-r}} \end{cases} \quad (27)$$

If $r < 1$ then $\mathcal{S}_{\bar{\tau},r}$ satisfies the IQC defined by the following multiplier Π_5:

$$\Pi_5(j\omega) := \begin{bmatrix} |\phi_5(j\omega)|^2 & 0 \\ 0 & -1 \end{bmatrix} \quad (28)$$

The proof that $\mathcal{S}_{\bar{\tau},r} \in \text{IQC}(\Pi_5)$ uses the bound $\|\mathcal{S}_{\bar{\tau},r} \circ \frac{1}{s}\| \leq \bar{\tau}$. The IQC multiplier Π_5 is analogous to the QC multiplier Π_2 provided in Example 2 for constant delays. Specifically, a Taylor series expansion for $\hat{\mathcal{S}}_{\bar{\tau}}$ can be used to show that Π_5 is equivalent to Π_2 at low frequencies. The bound on $|\phi_5|$ effectively increases the radius of circle constraints defined by Π_5 at high frequencies to account for the time variations and to cover all delays in $[0, \bar{\tau}]$. Note that as $r \to 0$, the high frequency bound in Π_5 becomes $|\phi_5(j\omega)| > 2$. Thus as $r \to 0$, Π_5 converges to the multipliers $\tilde{\Pi}_2$ used to cover all constant delays in $[0, \bar{\tau}]$. Again, these interpretations of Π_5 are imprecise and only meant to provide an intuitive interpretation. Proposition 3 in [19] gives a similar IQC multiplier that is valid for $r < 2$.

Example 6. Example 3 in Section IV-B provided a QC multiplier Π_3 for constant delays corresponding to a circle centered at $\frac{1}{2}\hat{\mathcal{S}}_{\tau}(j\omega)$. The benefit of this multiplier is that it defined a smaller circle than the multipliers given in Examples 1 and 2. This frequency domain intuition can be used to derive a new, related IQC for time-varying delays. The new IQC depends on a rational transfer function $\phi_6(s)$ that satisfies:

$$|\phi_6(j\omega)| > \begin{cases} \frac{1}{2}\bar{\tau}|\omega| & \text{if } \frac{1}{2}\bar{\tau}|\omega| \leq 1 + \frac{1}{\sqrt{1-r}} \\ 1 + \frac{1}{\sqrt{1-r}} & \text{if } \frac{1}{2}\bar{\tau}|\omega| > 1 + \frac{1}{\sqrt{1-r}} \end{cases} \quad (29)$$

It is shown in Appendix A that if $r < 1$ then $\mathcal{S}_{\bar{\tau},r}$ satisfies the IQC defined by the following multiplier Π_6:

$$\Pi_6(j\omega) := \begin{bmatrix} |\phi_6(j\omega)|^2 - \frac{1}{4}|\hat{\mathcal{S}}_{\bar{\tau}}(j\omega)|^2 & \frac{1}{2}\hat{\mathcal{S}}_{\bar{\tau}}(j\omega) \\ \frac{1}{2}\hat{\mathcal{S}}_{\bar{\tau}}(j\omega) & -1 \end{bmatrix} \quad (30)$$

The proof that $\mathcal{S}_{\bar{\tau},r} \in \text{IQC}(\Pi_6)$ uses the bound $\|(\mathcal{S}_{\bar{\tau},r} - \frac{1}{2}\mathcal{S}_{\bar{\tau}}) \circ \frac{1}{s}\| \leq \frac{1}{2}\bar{\tau}$. Again, a Taylor series expansion for $\hat{\mathcal{S}}_{\bar{\tau}}$ can be used to show that Π_6 is equivalent to the analogous multiplier for constant delays Π_3 at low frequencies. The bound on $|\phi_6|$ effectively increases the radius of circle constraints defined by Π_6 at high frequencies to account for the time variations and to cover all delays in $[0, \bar{\tau}]$.

Each of the multipliers can be generalized for the case where $\mathcal{S}_{\bar{\tau},r}$ is MIMO using the idea of scalings already introduced in Section IV-A. $\mathcal{S}_{\bar{\tau},r}$ is not a time-invariant system and hence frequency-dependent scalings cannot be used. However, the linearity of $\mathcal{S}_{\bar{\tau},r}$ can be used to show that constant matrix scalings can be introduced into the multiplier. For example, Π_4 remains a valid IQC multiplier for $\mathcal{S}_{\bar{\tau},r}$ if it is generalized to include any matrix $X \geq 0$:

$$\Pi_4 := \begin{bmatrix} \frac{r}{1-r}X & -X \\ -X & -X \end{bmatrix}. \quad (31)$$

A formal proof that $\mathcal{S}_{\bar{\tau},r} \in \text{IQC}(\Pi_4)$ is given in Proposition 1 of [19]. Reference [19] derives additional IQCs for time-varying delays. In particular, frequency-dependent scalings can be introduced into the multipliers for varying delays but, in this case, a swapping lemma must be used to account for the the time-variations in the delay. This section does not intend to provide an exhaustive review of IQCs for time-varying delays. Instead the main purpose is to demonstrate the benefit of the frequency-domain intuition provided by QCs for constant delays. Example 6 is a new IQC derived for time-varying delays using this intuition and it should be possible to derive additional useful IQCs using this approach.

V. TIME DOMAIN STABILITY ANALYSIS

The previous section defined frequency domain constraints that describe the input/output behavior of a time delay. These were specified as QCs for constant delays and IQCs for time-varying delays. This section shows that, under some mild technical conditions, these constraints have an equivalent time domain representation (Section V-A). The alternative time domain representation for QCs and IQCs is used to derive dissipation inequality based stability conditions for delayed nonlinear and parameter varying systems (Sections V-B and V-C).

A. Time Domain IQCs

Let Π be an QC or IQC multiplier that is a rational and uniformly bounded function of $j\omega$, i.e. $\Pi \in \mathbb{RL}_{\infty}^{(m_1+m_2)\times(m_1+m_2)}$. As noted previously QCs hold pointwise in frequency and hence they are also valid when integrated over frequency. In other words, if Π is a valid QC multiplier for a system Δ then it is also a valid IQC multiplier for the same system. Thus it is sufficient to provide a time domain interpretation for IQCs.

The time domain interpretation is based on factorizing the multiplier as $\Pi = \Psi^{\sim}M\Psi$ where $M = M^T \in \mathbb{R}^{n_z \times n_z}$ and $\Psi \in \mathbb{RH}_{\infty}^{n_z \times (m_1+m_2)}$. The restriction to rational, bounded multipliers Π ensures that such factorizations can be numerically computed via transfer function or state-space methods [43], [39], [23]. Such factorizations are not unique and two specific factorizations are provided in Appendix B using state-space methods. For a general factorization, Ψ is assumed to be stable but may be non-square ($n_z \neq m$) and possibly non-minimum phase.

Next, let (v, w) be a pair of signals that satisfy the IQC in (23) and define $\hat{z}(j\omega) := \Psi(j\omega) \begin{bmatrix} \hat{v}(j\omega) \\ \hat{w}(j\omega) \end{bmatrix}$. Then the IQC can be written as:

$$\int_{-\infty}^{\infty} \hat{z}(j\omega)^* M\hat{z}(j\omega) d\omega \geq 0 \tag{32}$$

By Parseval's theorem [45], this frequency-domain inequality can be equivalently expressed in the time-domain as:

$$\int_0^{\infty} z(t)^T M z(t)\, dt \geq 0 \tag{33}$$

where z is the output of the LTI system Ψ:

$$\begin{aligned} \dot{\psi}(t) &= A_\psi \psi(t) + B_{\psi 1} v(t) + B_{\psi 2} w(t), \quad \psi(0) = 0 \\ z(t) &= C_\psi \psi(t) + D_{\psi 1} v(t) + D_{\psi 2} w(t) \end{aligned} \tag{34}$$

Thus signals $v \in L_2^{m_1}[0, \infty)$ and $w \in L_2^{m_2}[0, \infty)$ satisfy the IQC defined by $\Pi = \Psi^\sim M \Psi$ if and only if the filtered signal $z = \Psi \begin{bmatrix} v \\ w \end{bmatrix}$ satisfies the time domain constraint in (33). Similarly, a bounded, causal system Δ satisfies the IQC defined by $\Pi = \Psi^\sim M \Psi$ if and only if (33) holds for all $v \in L_2^{m_1}[0, \infty)$ and $w = \Delta(v)$. To simplify notation, $\Delta \in \text{IQC}(\Pi)$ will also be denoted by $\Delta \in \text{IQC}(\Psi, M)$. Fig. 6 provides a graphical interpretation for this time-domain form of $\Delta \in \text{IQC}(\Psi, M)$. The input and output signals of Δ are filtered through Ψ and the output z satisfies the time-domain inequality in (33). A simple example is provided to illustrate the connection between the time domain and frequency domain constraints.
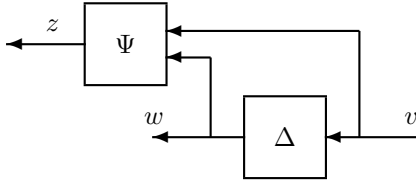

Fig. 6. Graphical interpretation of the IQC defined by $\Pi = \Psi^\sim M \Psi$

Example 7. Consider the multiplier $\bar{\Pi}_2(j\omega) = \begin{bmatrix} |\phi_2(j\omega)|^2 & 0 \\ 0 & -1 \end{bmatrix}$ (Equation 20) where ϕ_2 is a stable LTI system that satisfies certain bounds. This multiplier is a rational approximation that corresponds, at low frequencies, to a circle centered at the origin with a frequency-dependent radius. $\mathcal{S}_\tau \in \text{QC}(\bar{\Pi}_2)$ implies $\mathcal{S}_\tau \in \text{IQC}(\bar{\Pi}_2)$. Hence any $v = L_2[0, \infty)$ and $w = \mathcal{S}_\tau v$ satisfy

$$\int_{-\infty}^{\infty} \begin{bmatrix} \hat{v}(j\omega) \\ \hat{w}(j\omega) \end{bmatrix}^* \bar{\Pi}_2(j\omega) \begin{bmatrix} \hat{v}(j\omega) \\ \hat{w}(j\omega) \end{bmatrix} d\omega \geq 0 \tag{35}$$

A factorization for this multiplier is given by $M = \begin{bmatrix} 1 & 0 \\ 0 & -1 \end{bmatrix}$ and $\Psi = \begin{bmatrix} \phi_2(j\omega) & 0 \\ 0 & 1 \end{bmatrix}$. If $w = \mathcal{S}_\tau v$ then $z := \Psi \begin{bmatrix} v \\ w \end{bmatrix} = \begin{bmatrix} \phi_2 v \\ w \end{bmatrix}$. Hence the time-domain form for the IQC is

$$\int_0^{\infty} z(t)^T M z(t) = \int_0^{\infty} z_1^2(t) - z_2^2(t)\, dt \geq 0 \tag{36}$$

where $z_2 = w$ and $z_1 = \phi_2 v$. In other words, w has L_2 norm less than the filtered signal $\phi_2 v$, i.e. $\|w\| \leq \|\phi_2 v\|$.

It is important to note that the time domain constraint (33) holds, in general, only over infinite time intervals. The term hard IQC was introduced in [26] referring to the following more restrictive property: Δ satisfies the IQC defined by Π and $\int_0^T z(t)^T M z(t)\, dt \geq 0$ holds for all $T \geq 0$, $v \in L_{2e}^{m_1}[0, \infty)$ and $w = \Delta(v)$. By contrast, IQCs for which the time domain constraint need not hold over all finite time intervals are called soft IQCs. Hard and soft IQCs were later generalized in [25] to include the effect of initial conditions and the terms were renamed complete and conditional IQCs, respectively. The hard/soft terminology will be used here.

This distinction between hard and soft IQCs is important because the dissipation inequality theorems developed below require the use of time-domain constraints that hold over all finite-time intervals. One issue is that the factorization of Π as $\Psi^\sim M \Psi$ is not unique and hence there is ambiguity surrounding the hard/soft IQC terminology. As a result, the characterizations of hard and soft are not inherent to the IQC multiplier Π but instead depend on the factorization (Ψ, M). A more precise definition that refers to the factorization (Ψ, M) is now given.

Definition 4. Let Π be factorized as $\Psi^\sim M \Psi$ with Ψ stable. Then (Ψ, M) is a hard IQC factorization of Π if for any bounded, causal operator $\Delta \in \text{IQC}(\Pi)$ the following time-domain inequality holds

$$\int_0^T z(t)^T M z(t)\, dt \geq 0 \tag{37}$$

for all $T \geq 0$, $v \in L_2^{m_1}[0, \infty)$, $w = \Delta(v)$, and $z = \Psi \begin{bmatrix} v \\ w \end{bmatrix}$.

It was recently shown that a broad class of IQC multipliers have a hard factorization [24]. The proof uses a new min/max theorem to obtain a lower bound on $\int_0^T z(t)^T M z(t)\, dt$. A similar factorization result was obtained in [40] using a game-theoretic interpretation. The next theorem summarizes the main factorization result needed in order to use IQCs within the dissipation inequality framework.

Theorem 1. Let $\Pi = \Pi^\sim \in \mathbb{RL}_\infty^{(m_1+m_2) \times (m_1+m_2)}$ be partitioned as $\begin{bmatrix} \Pi_{11} & \Pi_{21}^\sim \\ \Pi_{21} & \Pi_{22} \end{bmatrix}$ where $\Pi_{11} \in \mathbb{RL}_\infty^{m_1 \times m_1}$ and $\Pi_{22} \in \mathbb{RL}_\infty^{m_2 \times m_2}$. Assume $\Pi_{11}(j\omega) > 0$ and $\Pi_{22}(j\omega) < 0$ for all $\omega \in \mathbb{R} \cup \{\infty\}$. Then Π has a hard factorization (Ψ, M).

Proof. The sign definite conditions on Π_{11} and Π_{22} ensure that Π has a factorization (M, Ψ) where Ψ is square and both Ψ, Ψ^{-1} are stable. This follows from Lemmas 4 and 5 in Appendix B. Moreover, Appendix B provides a numerical algorithm to compute this special (J-spectral) factorization using state-space methods. The conclusion that (M, Ψ) is a hard factorization follows from Theorem 2.4 in [24]. $\square$

B. Analysis of Nonlinear Delayed Systems

This section derives analysis conditions for the nonlinear delayed system $F_u(G, \mathcal{S}_\tau)$ shown in Fig. 2 using dissipation inequalities. For concreteness the discussion focuses on $\mathcal{S}_\tau$ defined with constant delays but the results also hold using IQCs valid for $\mathcal{S}_{\bar{\tau}, r}$ defined with varying delays. Assume $\mathcal{S}_\tau$

satisfies the IQC defined by Π and, in addition, Π has a hard factorization (Ψ, M). The feedback system can be analyzed using the interconnection structure shown in Fig. 7 with the system Ψ appended to the input/output channels of $\mathcal{S}_\tau$. The dynamics of the interconnection in Fig. 7 involve an extended system of the form

$$\dot{x} := F(x, w, d)$$
$$\begin{bmatrix} z \\ e \end{bmatrix} = H(x, w, d) \qquad (38)$$

$x := \begin{bmatrix} x_G \\ \psi \end{bmatrix} \in \mathbb{R}^{n_G + n_\psi}$ is the extended state and the functions F and H can be easily determined from the dynamics of G and Ψ. The theorem below provides a sufficient condition for the feedback interconnection to have an induced L_2 gain from d to e that is less than or equal to γ. The theorem is based on a dissipation inequality that uses both the hard IQC associated with $\mathcal{S}_\tau$ as well as a storage function V defined on the extended state x. The system $\mathcal{S}_\tau$ is shown as a dashed box in Fig. 7 because the analysis essentially replaces the precise relation $w = \mathcal{S}_\tau(v)$ with the hard IQC constraint on z that specifies the signals pairs (v, w) that are consistent with the behavior of $\mathcal{S}_\tau$.
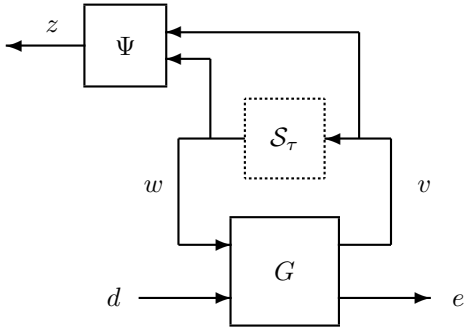

Fig. 7. Analysis Interconnection Structure

Theorem 2. Assume $F_u(G, \mathcal{S}_\tau)$ is well-posed and $\mathcal{S}_\tau$ satisfies the hard IQC defined by (Ψ, M). Then $\|F_u(G, \mathcal{S}_\tau)\| \leq \gamma$ if there exists a scalar $\lambda \geq 0$ and a continuously differentiable storage function $V : \mathbb{R}^{n_G + n_\psi} \to \mathbb{R}$ such that:

i) $V(0) = 0$,
ii) $V(x) \geq 0 \;\; \forall x \in \mathbb{R}^{n_G + n_\psi}$,
iii) The following dissipation inequality holds for all $x \in \mathbb{R}^{n_G + n_\psi}, w \in \mathbb{R}^{n_v}, d \in \mathbb{R}^{n_d}$

$$\lambda z^T M z + \nabla V(x) \cdot F(x, w, d) \leq \gamma^2 d^T d - e^T e \quad (39)$$

where z and e are functions of (x, w, d) as defined by H in Equation 38.

Proof. Let $d \in L_2^{n_d}[0, \infty)$ be any input signal. From well-posedness of the interconnection, the interconnection $F_u(G, \mathcal{S}_\tau)$ has a solution that satisfies the dynamics in Equation 38. The dissipation inequality (Equation 39) can be

integrated from $t = 0$ to $t = T$ with the initial condition $x(0) = 0$ to yield:

$$\lambda \int_0^T z(t)^T M z(t)\, dt + V(x(T)) \leq \gamma^2 \int_0^T d(t)^T d(t)\, dt \qquad (40)$$

$$- \int_0^T e(t)^T e(t)\, dt$$

It follows from the hard IQC condition, $\lambda \geq 0$, and the non-negativity of the storage function V that

$$\int_0^T e(t)^T e(t)\, dt \leq \gamma^2 \int_0^T d(t)^T d(t)\, dt \qquad (41)$$

Hence $\|F_u(G, \mathcal{S}_\tau)\| \leq \gamma$. $\qquad \square$

The dissipation inequality (Equation 39) is an algebraic constraint on variables (x, w, d). The dissipation inequality only depends on $\mathcal{S}_\tau$ via the constraint on $z^T M z$. Thus the dependence of the dissipation inequality on the delay value τ appears through the choice of the multiplier Π. Specifically, Π typically depends on the value of τ, e.g. Π_2 and Π_3 defined previously. The delay value is selected and then the multiplier Π and its hard factorization (Ψ, M) are constructed. Thus for a given delay value τ, Theorem 2 provides convex conditions on V, λ, and γ that are sufficient to upper bound the L_2 gain of $F_u(G, \mathcal{S}_\tau)$.

This leads to a useful numerical procedure if additional assumptions are made on G. If the dynamics of G (Equation 4) are described by polynomial vector fields then the functions F and H in the extended system are also polynomials. If the storage function V is also restricted to be polynomial then the dissipation inequality (Equation 39) and non-negativity condition $V \geq 0$ are simply global polynomial constraints. In this case the search for a feasible storage function V and scalars λ, γ can be formulated as a sum-of-squares (SOS) optimization [32], [33], [22]. For fixed delay τ this yields a convex optimization to upper bound the L_2 gain of $F_u(G, \mathcal{S}_\tau)$. In addition, bisection can be used to find the largest delay $\bar{\tau}$ such that the gain from d to e remains finite. If the QC multiplier Π covers $\mathcal{S}_\tau$ for all $\tau \in [0, \bar{\tau}]$ then $\bar{\tau}$ is a lower bound on the true delay margin. It is a lower bound because the dissipation inequality is only a sufficient condition. An example of this SOS method is given in Section VI-A. One issue with the SOS approach is that the required computation grows rapidly with the degree and number of variables contained in the polynomial constraint. This currently limits the proposed approach to situations where the extended system roughly involves a cubic vector field and state dimension less than $7 - 10$.

It should also be noted that the multiple IQCs can be incorporated in the analysis. Specifically, assume $\mathcal{S}_\tau$ satisfies the hard IQCs defined by (Ψ_k, M_k) for $k = 1, \cdots, N$. Each Ψ_k can be appended to the inputs/outputs of $\mathcal{S}_\tau$ to yield a filtered output z_k. Theorem 2 remains valid if the dissipation inequality (Equation 39) is modified to include the term $\sum_{k=1}^N \lambda_k z_k^T M_k z_k$ for any constants $\lambda_k \geq 0$. In this case the extended system includes the dynamics of G as well as the

dynamics of each Ψ_k ($k = 1, \cdots, N$). The stability analysis consists of a search for the storage V, gain bound γ, and the constants λ_k that lead to feasibility of the three conditions in Theorem 2. This approach enables many IQCs for $\mathcal{S}_\tau$ to be incorporated into the analysis.

C. Analysis of Parameter-Varying Delayed Systems

A similar analysis condition can be derived for parameter-varying delayed systems. In particular, Linear Parameter Varying (LPV) systems are a class of linear systems whose state space matrices depend on a time-varying parameter vector $\rho : \mathbb{R}^+ \to \mathbb{R}^{n_\rho}$. The parameter is assumed to be a continuously differentiable function of time and admissible trajectories are restricted, based on physical considerations, to a known compact subset $\mathcal{P} \subset \mathbb{R}^{n_\rho}$. The state-space matrices of an LPV system are continuous functions of the parameter, e.g. $A_G : \mathcal{P} \to \mathbb{R}^{n_x \times n_x}$. Define the LPV system G_ρ with inputs (w, d) and outputs (v, e) as:

$$
\begin{aligned}
\dot{x}_G(t) &= A_G(\rho(t))x_G(t) + B_G(\rho(t)) \begin{bmatrix} w(t) \\ d(t) \end{bmatrix} \\
\begin{bmatrix} v(t) \\ e(t) \end{bmatrix} &= C_G(\rho(t))x_G(t) + D_G(\rho(t)) \begin{bmatrix} w(t) \\ d(t) \end{bmatrix}
\end{aligned}
\tag{42}
$$

The state matrices at time t depend on the parameter vector at time t. Hence, LPV systems represent a special class of time-varying systems. Throughout this section the explicit dependence on t is occasionally suppressed to shorten the notation.

By loop-shifting, a delayed LPV system can be modeled as $F_u(G_\rho, \mathcal{S}_\tau)$ where $w = \mathcal{S}_\tau(v)$. This is similar to the interconnection shown in Figure 2 but with G_ρ as the "nominal" system. As a slight abuse of notation, $\|F_u(G_\rho, \mathcal{S}_\tau)\|$ will denote the worst-case L_2 gain over all allowable parameter trajectories:

$$
\|F_u(G_\rho, \mathcal{S}_\tau)\| = \sup_{\rho \in \mathcal{P}} \sup_{0 \neq d \in L_2^{n_d}[0,\infty), \ x_G(0)=0} \frac{\|e\|}{\|d\|}
\tag{43}
$$

As in the previous subsection, assume $\mathcal{S}_\tau$ satisfies the IQC defined by Π and that Π has a hard factorization (Ψ, M). The stability and performance of $F_u(G_\rho, \mathcal{S}_\tau)$ can be assessed by appending the system Ψ to the input/output channels of $\mathcal{S}_\tau$ (as in Fig. 7). The dynamics of the interconnection in Fig. 7 depend on an extended LPV system of the form:

$$
\begin{aligned}
\dot{x} &= A(\rho)x + B_1(\rho)w + B_2(\rho)d \\
z &= C_1(\rho)x + D_{11}(\rho)w + D_{12}(\rho)d \\
e &= C_2(\rho)x + D_{21}(\rho)w + D_{22}(\rho)d,
\end{aligned}
\tag{44}
$$

where the state vector is $x := \begin{bmatrix} x_G \\ \psi \end{bmatrix} \in \mathbb{R}^{n_G + n_\psi}$ with x_G and ψ denoting the state vectors of the LPV system G_ρ (Equation 42) and the filter Ψ (Equation 34), respectively. A dissipation inequality can be formulated to upper bound the worst-case L_2 gain of $F_u(G_\rho, \mathcal{S}_\tau)$ using the system (44) and the time domain IQC (37). This dissipation inequality is concretely expressed as a linear matrix inequality in the following theorem. The theorem is stated assuming a single multiplier Π for $\mathcal{S}_\tau$ but many IQC multipliers can be included as described in the previous section.

Theorem 3. Assume $F_u(G_\rho, \mathcal{S}_\tau)$ is well posed and $\mathcal{S}_\tau$ satisfies the hard IQC defined by (Ψ, M). Then $\|F_u(G_\rho, \mathcal{S}_\tau)\| \leq \gamma$ if there exists a scalar $\lambda \geq 0$ and a matrix $P = P^T \in \mathbb{R}^{n_x + n_\psi}$ such that $P \geq 0$ and for all $\rho \in \mathcal{P}$:

$$
\begin{aligned}
&\begin{bmatrix} A^T P + PA & PB_1 & PB_2 \\ B_1^T P & 0 & 0 \\ B_2^T P & 0 & -\gamma^2 I \end{bmatrix} + \begin{bmatrix} C_2^T \\ D_{21}^T \\ D_{22}^T \end{bmatrix} \begin{bmatrix} C_2 & D_{21} & D_{22} \end{bmatrix} \\
&\quad + \lambda \begin{bmatrix} C_1^T \\ D_{11}^T \\ D_{12}^T \end{bmatrix} M \begin{bmatrix} C_1 & D_{11} & D_{12} \end{bmatrix} < 0
\end{aligned}
\tag{45}
$$

In (45) the dependency of the state space matrices on ρ has been omitted to shorten the notation.

Proof. Define a storage function $V : R^{n_x + n_\psi} \to \mathbb{R}^+$ by $V(x) = x^T Px$. Left and right multiply (45) by $[x^T, w^T, d^T]$ and $[x^T, w^T, d^T]^T$ to show that V satisfies the dissipation inequality:

$$
\lambda z(t)^T M z(t) + \dot{V}(t) \leq \gamma^2 d(t)^T d(t) - e(t)^T e(t)
\tag{46}
$$

The remainder of the proof is similar to that given for Theorem 2. $\qquad \square$

The analysis of the delayed LPV system reduces to a set of parameter dependent LMIs. These are infinite dimensional and hence they are typically approximated by finite-dimensional LMIs evaluated on a grid of parameter values. In this case the search for the matrix P and scalars λ, γ can be performed as a semidefinite programming optimization [4]. If the LPV system has a rational dependence on the parameters then a finite dimensional LMI condition can be derived (with no approximation) using the techniques in [28], [1]. In addition, there may be known bounds on the parameter rates of variation. Theorem 3 does not incorporate such knowledge and hence this is called a rate-unbounded analysis condition. Theorem 3 can be easily extended to include rate-bounds using parameter-dependent storage functions as described in [42]. Finally, if the system G_ρ is LTI then Equation 46 reduces to a single LMI condition. The nonlinear dissipation inequality in Theorem 2 is equivalent to exactly the same LMI condition when G is LTI and V is a quadratic function of x. In other words, Theorems 2 and 3 are the same for LTI dynamics and quadratic storage functions.

VI. NUMERICAL EXAMPLES

This section presents numerical examples to assess the stability and performance for nonlinear and LPV delayed systems.

A. Nonlinear Delayed System

Consider the classical feedback loop shown in Fig. 8 where $\mathcal{D}_\tau$ is a constant delay. L is a nonlinear system described by the following ODE:

$$\dot{x}_G = \begin{bmatrix} -49 & 0 \\ 1 & 0 \end{bmatrix} x_G + \begin{bmatrix} 8 \\ 0 \end{bmatrix} \tilde{w} + p(x_G)$$

$$y = \begin{bmatrix} -4.5 & 1.5 \end{bmatrix} x_G$$

(47)

where $p(x_G) := \begin{bmatrix} 2x_{G,1}^2 + 3x_{G,2}^2 - 0.2x_{G,1}^3, & -x_{G,2}^3 \end{bmatrix}^T$. As described in Section III, a loop-shift can be performed to bring the classical feedback loop into the form $F_u(G, \mathcal{S}_\tau)$ shown in Fig. 2.
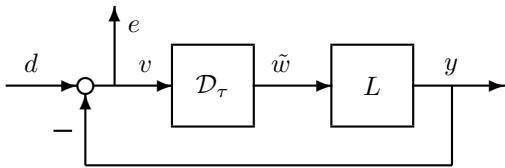

Fig. 8. Classical Feedback Loop

First, a linear analysis is performed to gain insight into the use of QCs for analysis. Let G_{lin} denote the linearization of G around $x_G = 0$. This linearization is obtained by neglecting the higher order terms in (47), i.e. neglecting $p(x_G)$. An estimate for the delay margin of $F_u(G_{lin}, \mathcal{S}_\tau)$ can be computed from the LMI condition in Theorem 3. Bisection is used to find the largest time delay for which the gain from d to e is finite. A number of solvers exist for this class of systems and here the Matlab `LMILab` toolbox was used. Using the standard multipliers Π_1 and $\bar{\Pi}_2$ gives a delay margin of 0.06sec. However, using the multipliers Π_1 and the new "small" circle multiplier $\bar{\Pi}_3$ yields a significantly larger delay margin estimate of 1.96sec. The exact delay margin for $F_u(G_{lin}, \mathcal{S}_\tau)$ can be estimated from the frequency response of G_{lin}. The frequency response gives a delay margin of 2.05 sec with a critical frequency 0.361 rad/sec. These results are summarized in Tab. I.

System	Method	Delay Margin
Linear, G_{lin}	IQC with Π_1 and $\bar{\Pi}_2$	0.06sec
Linear, G_{lin}	IQC with Π_1 and $\bar{\Pi}_3$	1.96sec
Linear, G_{lin}	Frequency Response	2.05 sec
Nonlinear, G	IQC with Π_1 and $\bar{\Pi}_3$	1.09sec

TABLE I
SUMMARY OF DELAY MARGINS

The results can be interpreted in the complex plane as shown in Fig. 9. The figure shows the circle constraints described by $\bar{\Pi}_1$ and $\bar{\Pi}_3$ at the critical frequency 0.361 rad/sec (dotted blue). The figure also shows the circle described by the optimal multiplier $\Pi_{opt} := \lambda_1 \Pi_1 + \lambda_3 \bar{\Pi}_3$ (solid blue). The coefficients in the optimal conic combination are given by $\lambda_1 = 5310$ and $\lambda_3 = 7210$. Finally, the figure shows the location of $\hat{\mathcal{S}}_\tau(j\omega) = e^{-j\omega\tau} - 1$ evaluated at the critical

frequency and delay margin estimate of $\tau = 1.96$ sec (small red circle). The location of $\hat{\mathcal{S}}_\tau$ lies inside the circle described by Π_{opt} at the critical frequency. In fact, $\hat{\mathcal{S}}_\tau$ lies inside the circle described by Π_{opt} at all frequencies. This is consistent with the following rough frequency-domain interpretation of the dissipation inequality result: $F_u(G, \Delta)$ is stable for LTI perturbations Δ whose Nyquist plot lies within the circles described Π_{opt}.
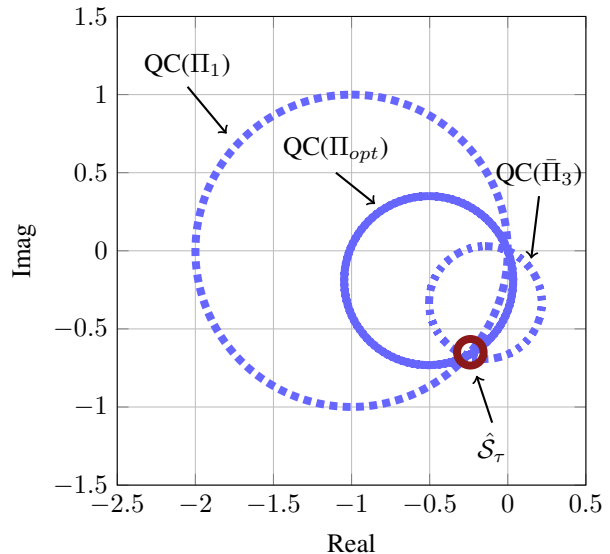

Fig. 9. Nyquist plot showing quadratic constraints.

This frequency domain interpretation can also be used to explain the poor delay margin bound obtained with Π_1 and $\bar{\Pi}_2$. Briefly, the transfer function from w to v (upper left corner of G_{lin}) is given by $-T = \frac{-L_{lin}(s)}{1+L_{lin}(s)}$, i.e. the negative complementary sensitivity function. Standard robust control techniques [41] can be used to show that $\Delta := \frac{-1}{T(j\omega_0)}$ is a complex perturbation that causes $F_u(G_{lin}, \Delta)$ to have poles at $\pm j\omega_0$. At high frequencies these "small" destabilizing perturbations follow a vertical line in the complex plane with real part equal to 0.37. This constrains the use of $\bar{\Pi}_2$ because this multiplier defines a circle centered at the origin with radius greater than $\hat{\mathcal{S}}_\tau$. The destabilizing perturbations lie within this circle unless the time delay is chosen to be small. This issue can be eliminated by frequency weighting the multiplier $\bar{\Pi}_2$, e.g. weighting each entry by $\left| \frac{s+1}{10s+1} \right|^2$. However, this increases the state order of the multiplier and hence the computation time.

Next consider the analysis of the delayed nonlinear system. An estimate for the delay margin of $F_u(G, \mathcal{S}_\tau)$ can be computed from the dissipation inequality in Theorem 2. A number of solvers exist for the corresponding sum-of-squares optimizations. Here the SOSOPT toolbox [2] was used for all computations. Using the multipliers Π_1 and $\bar{\Pi}_3$ yields a delay margin of $\bar{\tau}_{NL} = 1.09$ sec for the nonlinear system. Thus the nonlinearities significantly degrade the delay margin bound. The bisection was initialized with the bounds $\bar{\tau}_{NL} \in [0, 5]$. The computation took 5.2 secs to perform 13 bisection steps to achieve a tolerance of 0.001.
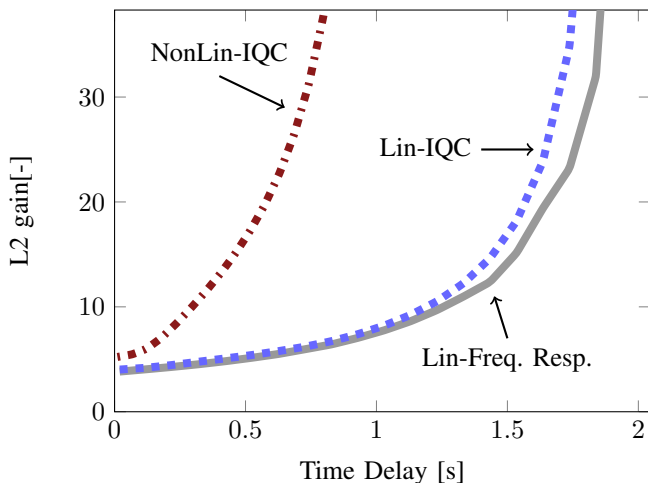
Fig. 10. Induced L_2 gain versus delay

The L_2 gain of the delayed nonlinear system from reference d to tracking error e can also be computed from the dissipation inequality in Theorem 2. Figure 10 shows the gain of the nonlinear system for delays below the delay margin estimate, $\tau < \bar{\tau}_{NL} = 1.09$ sec (green dash-dot). The multipliers Π_1 and $\bar{\Pi}_3$ were used to compute this curve. It took 7.5 sec to evaluate the gain on a grid of 20 delay values. For comparison the figure also shows the gain of the linear system $F_u(G_{lin}, \mathcal{S}_\tau)$ computed using two methods. The red dashed curve is the gain computed using the LMI condition in Theorem 3 also with multipliers Π_1 and $\bar{\Pi}_3$. The blue solid curve is the true induced L_2 gain of the linear system estimated from the frequency response of $F_u(G_{lin}, \mathcal{S}_\tau)$. The two linear results are close which provides confidence in the upper bounds computed via the IQC and dissipation inequality condition. The figure also shows that the nonlinear delayed system has significantly larger gain as compared to the linearized system. This again indicates that the nonlinearities significantly degrade the performance.

B. LPV Delayed System

The second example is an LPV time-delayed system representing a cutter used in milling. The system G_ρ, taken from [44], can be written as

$$
\dot{x}_G = \begin{bmatrix} 0 & & 0 & 1 & 0 \\ 0 & & 0 & 0 & 1 \\ -(10 + 0.171k) + 0.5k\rho & 10 & 0 & 0 \\ 5 & & -15 & 0 & -0.25 \end{bmatrix} x_G
$$
$$
+ \begin{bmatrix} 0 & 0 & 0 & 0 \\ 0 & 0 & 0 & 0 \\ 0.171k - 0.5k\rho & 0 & 0 & 0 \\ 0 & 0 & 0 & 0 \end{bmatrix} \tilde{w}
$$
$$
\tilde{w} = \mathcal{D}_\tau(x_G)
$$

(48)

where k is the cutting stiffness and $\rho \in [-1, 1]$ is an artificial scheduling parameter depending on the angular position of the

blade. Since G_ρ only depends affinely on the parameter ρ, it is sufficient to only consider the vertices, i.e. $\rho = -1$ and $\rho = 1$, for the following analyses. The goal of the benchmark is to find the time delay margin of the plant for a given cutting stiffness k. As in the previous example a loop shift is performed to bring the system into the form $F_u(G_\rho, \mathcal{S}_\tau)$.

The results of the analysis are shown in Fig. 11. The IQC approach is based on the LMI condition Theorem 3 and solved via bisection using the Matlab `LMILab` toolbox. The IQC analysis is performed using the combination of multipliers Π_1 and $\bar{\Pi}_2$. The IQC analysis is also performed using Π_1 and $\bar{\Pi}_3$. Finally the method from [44] based on Lyapunov-Krasovskii functionals is shown for comparison with the IQC approach. It is shown in [44] that the system is stable independent of the delay for stiffness values $k \leq 0.267$. As can be seen in the figure, all three methods capture this behavior well. For higher stiffness values, the IQC method with using multipliers Π_1 and $\bar{\Pi}_3$ yields improved margin bounds as compared to the analysis condition from [44]. It should be noted that the improved Lyapunov-Krasovskii condition in [15] achieves results similar to the best IQC results obtained with Π_1 and $\bar{\Pi}_3$.
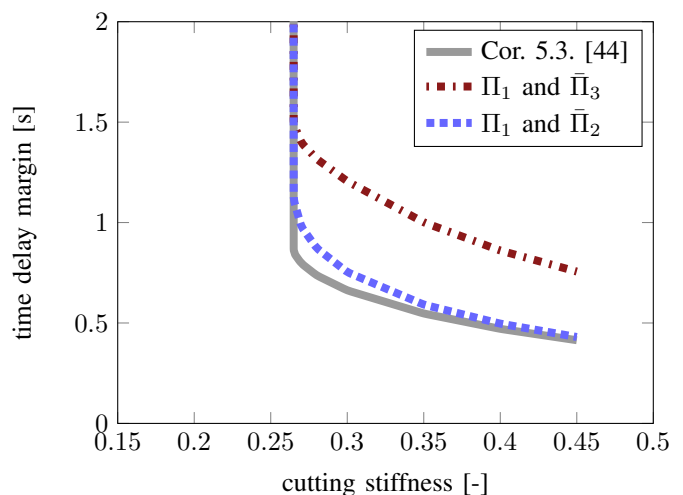

Fig. 11. Time Delay Margin vs Cutting Stiffness

VII. CONCLUSIONS

This paper developed stability and performance analysis conditions for nonlinear and LPV time-delayed systems. The approach bounds the behavior of the time delay using integral quadratic constraints (IQCs). IQCs are typically specified as frequency domain constraints on the inputs and outputs of an operator. For constant time delays, such IQCs were shown to have an intuitive geometric interpretation at each frequency. This intuition led to the construction of new IQCs for both constant and varying delays. Dissipation inequalities were then provided that incorporate IQCs into the analysis of delayed systems. This analysis approach applied existing results to obtain an equivalent time-domain interpetation for IQCs. Finally, numerical examples were provided to demonstrate the proposed methods. While this paper only considers a single time delay, the framework can easily incorporate additional

delays and uncertainties analysis. Future work will explore the connections between the IQCs/dissipation inequality approach and standard Lyapunov methods.

ACKNOWLEDGMENTS

REFERENCES

[1] P. Apkarian and P. Gahinet. A convex characterization of gain-scheduled H_∞ controllers. *IEEE Trans. on Automatic Control*, 40:853–864, 1995.

[2] G.J. Balas, A. Packard, P. Seiler, and U. Topcu. SOSOPT toolbox and user's guide. http://www.aem.umn.edu/~AerospaceControl/, 2013.

[3] H. Bart, I. Gohberg, and M.A. Kaashoek. *Minimal Factorization of Matrix and Operator Functions*. Birkhäuser, Basel, 1979.

[4] S. Boyd, L. El Ghaoui, E. Feron, and V. Balakrishnan. *Linear Matrix Inequalities in System and Control Theory*, volume 15 of *Studies in Applied Mathematics*. SIAM, Philadelphia, 1994.

[5] Corentin Briat. *Linear Parameter-Varying and Time-Delay Systems*. Springer, Heidelberg, 2014.

[6] J. Doyle. Analysis of feedback systems with structured uncertainties. *Proc. of IEE*, 129-D:242–251, 1982.

[7] J.C. Doyle. Structured uncertainty in control system design. In *Proc. of the Conference on Decision and Control*, pages 260–265, 1985.

[8] G. Dullerud and F. Paganini. *A Course in Robust Control Theory: A Convex Approach*. Springer, New York, 1999.

[9] M.K.H. Fan, A.L. Tits, and J.C. Doyle. Robustness in the presence of mixed parametric uncertainty and unmodeled dynamics. *IEEE Trans. On Automatic Control*, 36(1):25–38, 1991.

[10] A.L. Fradkov and V.A. Yakubovich. The S-procedure and a duality relation in nonconvex problems of quadratic programming. *Vestnik Leningrad Univ. Math.*, 5(1):101–109, 1979.

[11] B. Francis. *A Course in H_∞ Control Theory*. Springer-Verlag, New York, 1987.

[12] E. Fridman and U. Shaked. An improved stabilization method for linear time-delay systems. *IEEE Trans. on Automatic Control*, 47(11):1931–1937, 2002.

[13] M. Fu, H. Li, and S. Niculescu. *Stability and Control of Time Delay Systems*, chapter Robust stability and stabilization of time-delay systems via integral quadratic constraint approach, pages 101–116. Springer, London, 1997. L. Dugard and E.I. Verriest (Editors).

[14] M. Green, K. Glover, D.J.N. Limebeer, and J.C. Doyle. A J-spectral factorization approach to H_∞ control. *SIAM Journal of Control and Optimization*, 28(6):1350–1371, 1990.

[15] K. Gu. Discretized LMI set in the stability problem of linear uncertain time-delay systems. *Int. Journal of Control*, 68(4):923–934, 1997.

[16] K. Gu, V. Kharitonov, and J. Chen. *Stability of Time-Delay Systems*. Birkhäuser, Basel, 2002.

[17] U.T. Jönsson. A lecture on the S-procedure. Lecture Notes, 2006.

[18] C.Y. Kao and B. Lincoln. Simple stability criteria for systems with time-varying delays. *Automatica*, 40:1429–1434, 2004.

[19] C.Y. Kao and A. Rantzer. Stability analysis of systems with uncertain time-varying delays. *Automatica*, 43(6):959–970, 2007.

[20] H. Kimura. (J,J')-lossless factorization based on conjugation. *Systems and Control Letters*, 19:95–109, 1992.

[21] I.E. Kose and C. Scherer. Robust L2-gain feedforward control of uncertain systems using dynamic IQCs. *Int. Journal of Robust and Nonlinear Control*, 19(11):1224–1247, 2009.

[22] J.B. Lasserre. Global optimization with polynomials and the problem of moments. *SIAM Journal on Optim.*, 11(3):796–817, 2001.

[23] D. Materassi and M.V. Salapaka. Less conservative absolute stability criteria using integral quadratic constraints. In *American Control Conference*, pages 113–118, 2009.

[24] A. Megretski. KYP lemma for non-strict inequalities and the associated minimax theorem. arXiv, 2010.

[25] A. Megretski, U.T. Jönsson, C.Y. Kao, and A. Rantzer. *Control Systems Handbook*, chapter Chapter 41: Integral Quadratic Constraints. CRC Press, Boca Raton, 2010.

[26] A. Megretski and A. Rantzer. System analysis via integral quadratic constraints. *IEEE Trans. on Automatic Control*, 42:819–830, 1997.

[27] G. Meinsma. J-spectral factorization and equalizing vectors. *Systems and Control Letters*, 25:243–249, 1995.

[28] A. Packard. Gain scheduling via linear fractional transformations. *Systems and Control Letters*, 22:79–92, 1994.

[29] A. Packard and J. Doyle. The complex structured singular value. *Automatica*, 29:71–109, 1993.

[30] A. Papachristodoulou. Analysis of nonlinear time-delay systems using the sum of squares decomposition. In *American Control Conference*, volume 5, pages 4153–4158, 2004.

[31] A. Papachristodoulou, M. Peet, and S. Lall. Analysis of polynomial systems with time delays via the sum of squares decomposition. *IEEE Trans. on Automatic Control*, 54(5):1058–1064, 2009.

[32] P. Parrilo. *Structured Semidefinite Programs and Semialgebraic Geometry Methods in Robustness and Optimization*. PhD thesis, California Institute of Technology, 2000.

[33] P. Parrilo. Semidefinite programming relaxations for semialgebraic problems. *Mathematical Prog. Ser. B*, 96(2):293–320, 2003.

[34] M. Peet and S. Lall. Global stability analysis of a nonlinear model of internet congestion control with delay. *Automatic Control, IEEE Transactions on*, 52(3):553–559, March 2007.

[35] H. Pfifer and P. Seiler. Integral quadratic constraints for delayed nonlinear and parameter-varying systems. *accepted to Automatica*, 2014.

[36] H. Pfifer and P. Seiler. Robustness analysis of linear parameter varying systems using integral quadratic constraints. In *American Control Conference*, 2014.

[37] M.G. Safonov. *Stability and Robustness of Multivariable Feedback Systems*. MIT Press, 1980.

[38] C. Scherer and I.E. Kose. Gain-scheduled control synthesis using dynamic D-scales. *IEEE Trans. on Automatic Control*, 57:2219–2234, 2012.

[39] C. Scherer and S. Wieland. Linear matrix inequalities in control. Lecture notes for a course of the Dutch institute of systems and control, Delft University of Technology, 2004.

[40] P. Seiler. Stability analysis with dissipation inequalities and integral quadratic constraints. *accepted to the IEEE Trans. on Automatic Control*, 2014.

[41] S. Skogestad and I. Postlethwaite. *Multivariable Feedback Control*. John Wiley and Sons, Chichester, 2005.

[42] F. Wu, X. H. Yang, A. Packard, and G. Becker. Induced $\mathcal{L}_2$ norm control for LPV systems with bounded parameter variation rates. *Int. Journal of Robust and Nonlinear Control*, 6:983–998, 1996.

[43] D.C. Youla. On the factorization of rational matrices. *IRE Trans. on Information Theory*, 7(3):172–189, 1961.

[44] X. Zhang, P. Tsiotras, and C. Knospe. Stability analysis of LPV time-delayed systems. *Int. Journal of Control*, 75(7):538–558, 2002.

[45] K. Zhou, J.C. Doyle, and K. Glover. *Robust and Optimal Control*. Prentice-Hall, New Jersey, 1996.

APPENDIX

A. Time-varying IQC

This appendix provides a proof that if $r < 1$ then $\mathcal{S}_{\bar{\tau},r} \in$ IQC(Π_6) where the multiplier Π_6 is defined in Section IV-C. Two preliminary lemmas are required to prove this result.

Lemma 2. If $r < 1$ then $\|\mathcal{S}_{\bar{\tau},r} - \frac{1}{2}\mathcal{S}_{\bar{\tau}}\| \leq 1 + \frac{1}{\sqrt{1-r}}$.

Proof. Apply the triangle inequality as well as the definitions of $\mathcal{S}_{\bar{\tau},r}$ and $\mathcal{S}_{\bar{\tau}}$ to obtain the following bound:

$$\left\|\mathcal{S}_{\bar{\tau},r} - \frac{1}{2}\mathcal{S}_{\bar{\tau}}\right\| \leq \|\mathcal{D}_{\bar{\tau},r}\| + \frac{1}{2}\|\mathcal{D}_{\bar{\tau}}\| + \frac{1}{2} \tag{49}$$

The varying delay is bounded as $\|\mathcal{D}_{\bar{\tau},r}\| \leq \frac{1}{\sqrt{1-r}}$ [16], [19] while the constant delay is bounded by $\|\mathcal{D}_{\bar{\tau}}\| \leq 1$. $\qquad\square$

Lemma 3. $\|(\mathcal{S}_{\bar{\tau},r} - \frac{1}{2}\mathcal{S}_{\bar{\tau}}) \circ \frac{1}{s}\| \leq \frac{1}{2}\bar{\tau}$.

Proof. The proof is only sketched as it is similar to that given for Lemma 1 in [18]. To simplify notation define $\Delta := (\mathcal{S}_{\bar{\tau},r} - \frac{1}{2}\mathcal{S}_{\bar{\tau}}) \circ \frac{1}{s}$. Consider $w = \Delta v$ for some $v \in L_2[0, \infty)$ and define $y(t) := \int_0^t v(\alpha)d\alpha$. Thus $w = (\mathcal{S}_{\bar{\tau},r} - \frac{1}{2}\mathcal{S}_{\bar{\tau}})(y)$ which, after some algebra, gives

$$w(t) = \int_{t-\bar{\tau}}^t s(\alpha)v(\alpha)d\alpha \qquad (50)$$

where $s(\alpha) = +\frac{1}{2}$ for $\alpha \in [t-\bar{\tau}, t-\tau(t)]$ and $s(\alpha) = -\frac{1}{2}$ for $\alpha \in [t-\tau(t), t]$. The Cauchy-Schwartz inequality can then be used to show

$$w(t)^2 \leq \frac{\bar{\tau}}{4} \int_{t-\bar{t}}^t v^2(\alpha)d\alpha \qquad (51)$$

Integrate this inequality from $t = 0$ to $t = \infty$ and perform a change of variables to obtain $\|w\|^2 \leq \frac{\bar{\tau}^2}{4}\|v\|^2$. $\qquad\square$

Theorem 4. Let $\phi_6(s)$ be the transfer function defined in Equation 29. If $r < 1$ then $\|(\mathcal{S}_{\bar{\tau},r} - \frac{1}{2}\mathcal{S}_{\bar{\tau}}) \circ \phi_6^{-1}\| \leq 1$.

Proof. The proof is only sketched as it is essentially the same as that given for Proposition 2 in [19]. Let $v \in L_2$ be an input signal and $\hat{v} := \mathcal{F}(v)$ its corresponding Fourier Transform. Decompose v as $v_L + v_H$ where v_L and v_H are the low and high frequency components, respectively. Specifically, the low-frequency content is defined in the frequency domain by $\hat{v}_L(j\omega) := \hat{v}(j\omega)$ if $|\omega| \leq \frac{2}{\bar{\tau}}\left(1 + \frac{1}{\sqrt{1-r}}\right)$ and $\hat{v}_L(j\omega) := 0$ otherwise. The high-frequency content is defined similarly. To simplify notation, define $\Delta = (\mathcal{S}_{\bar{\tau},r} - \frac{1}{2}\mathcal{S}_{\bar{\tau}}) \circ \phi_6^{-1}$. Then using the linearity of Δ and the triangle inequality yields

$$\|\Delta v\| \leq \|\Delta v_L\| + \|\Delta v_H\| \qquad (52)$$

Lemmas 2 and 3 bound the gains on the high and low frequency components by $\|\Delta v_H\| \leq \|v_H\|$ and $\|\Delta v_L\| \leq \|v_L\|$. Thus $\|\Delta v\| \leq \|v_L\| + \|v_H\| = \|v\|$. $\qquad\square$

The bound in Theorem 4 can be equivalently expressed as a quadratic, frequency-domain constraint on the input/output signals of $\mathcal{S}_{\bar{\tau},r}$. This gives the desired result that $\mathcal{S}_{\bar{\tau},r}$ satisfies the IQC defined by the multiplier Π_6.

B. IQC Factorizations

This appendix provides specific numerical procedures to factorize $\Pi = \Pi^{\sim} \in \mathbb{RL}_{\infty}^{m \times m}$ as $\Psi^{\sim} M \Psi$. Such factorizations are not unique and this appendix presents two useful factorizations.

First, let $(A_\pi, B_\pi, C_\pi, D_\pi)$ be a minimal state-space realization for Π. Separate Π into its stable and unstable parts $\Pi = G_S + G_U$. Let (A, B, C, D_π) denote a state space realization for the stable part G_S. The matrix A is Hurwitz since G_S is stable. The assumptions on Π can be used to show that the poles of Π are symmetric about the imaginary axis

and, moreover, G_U has a state space realization of the form $(-A^T, -C^T, B^T, 0)$ (Section 7.3 of [11]). Thus $\Pi = G_S + G_U$ can be written in the form $\Pi = \Psi^{\sim} M \Psi$ where

$$\Psi(s) := \begin{bmatrix} (sI - A)^{-1}B \\ I \end{bmatrix} \qquad (53)$$

$$M := \begin{bmatrix} 0 & C^T \\ C & D_\pi \end{bmatrix} \qquad (54)$$

This provides a factorization $\Pi = \Psi^{\sim} M \Psi$ where $M = M^T \in \mathbb{R}^{n_z \times n_z}$ and $\Psi \in \mathbb{RH}_{\infty}^{n_z \times m}$. For this factorization Ψ is, in general, non-square ($n_z \neq m$) and it may have right-half plane zeros.

The stability theorems in this paper require a special factorization such that Ψ is square ($n_z = m$), stable, and minimum phase. More precisely, given non-negative integers p and q, let $J_{p,q}$ denote the signature matrix $\begin{bmatrix} I_p & 0 \\ 0 & -I_q \end{bmatrix}$. Ψ is called a $J_{p,q}$-spectral factor of Π if $\Pi = \Psi^{\sim} J_{p,q} \Psi$ and $\Psi, \Psi^{-1} \in \mathbb{RH}_{\infty}^{m \times m}$. The term J-spectral factor will be used if the values of p and q are not important. J-spectral factorizations have been used to construct (sub-optimal) solutions to the H_∞ optimal control problem [14], [20], [11]. The next lemma provides a necessary and sufficient condition for constructing a J-spectral factorization of Π.

Lemma 4. Let $\Pi \in \mathbb{RL}_{\infty}^{m \times m}$ be a multiplier in the form:

$$\Pi(s) = \begin{bmatrix} (sI - A)^{-1}B \\ I \end{bmatrix}^{\sim} \begin{bmatrix} 0 & C^T \\ C & D_\pi \end{bmatrix} \begin{bmatrix} (sI - A)^{-1}B \\ I \end{bmatrix} \qquad (55)$$

where A is Hurwitz. The following statements are equivalent:

1) $D_\pi = D_\pi^T$ is nonsingular and there exists a unique real solution $X = X^T$ to the following ARE

$$A^T X + XA - (XB + C^T)D_\pi^{-1}(B^T X + C) = 0 \qquad (56)$$

   such that $A - BD_\pi^{-1}(B^T X + C)$ is Hurwitz.

2) Π has a $J_{p,q}$ spectral factorization where p and q are the number of positive and negative eigenvalues of D_π, respectively. Moreover, Ψ is a $J_{p,q}$-spectral factor of Π if and only if it has a state-space realization $\left(A, B, J_{p,q}W^{-T}(B^T X + C), W\right)$ where W is a solution of $D_\pi = W^T J_{p,q} W$.

Proof. This lemma is based on the canonical factorization results in [3] and summarized in Chapter 7 of [11]. The precise wording of this lemma is a special case of Theorem 2.4 in [27]. $\qquad\square$

The numerical procedure to construct a J-spectral factorization of $\Pi = \Pi^{\sim}$ can be summarized by the following steps. First, express Π with a minimal realization $(A_\pi, B_\pi, C_\pi, D_\pi)$. Second, compute a state space realization (A, B, C, D_π) for the stable part of Π. This step can be done using the Matlab command `stabsep`. Third, attempt to solve for the stabilizing solution $X = X^T$ of the ARE in Equation 56. This step can be done using the Matlab command `care`. The existence of a stabilizing solution is related to the eigenvalues/eigenspaces

of a related Hamiltonian matrix (see [45]). If this step is unsuccessful, i.e. no such solution exists, then Π does not have a J-spectral factorization by Lemma 4. However, if the ARE has a unique stabilizing solution then construct the state-space realization for Ψ as defined in Statement 2) of Lemma 4. This requires the matrix decomposition $D_\pi = W^T J_{p,q} W$ which can be computed from an eigenvalue decomposition of D_π. This entire procedure, if successful, yields the factorization $\Pi = \Psi^\sim M \Psi$ where $M := J_{p,q}$ and $\Psi, \Psi^{-1} \in \mathbb{RH}_\infty^{m \times m}$.

The last result of this appendix provides a simple frequency domain condition that is sufficient for the existence of a J-spectral factor of a multiplier $\Pi = \Pi^\sim$.

Lemma 5. Let $\Pi = \Pi^\sim \in \mathbb{RL}_\infty^{(m_1+m_2) \times (m_1+m_2)}$ be partitioned as $\begin{bmatrix} \Pi_{11} & \Pi_{12} \\ \Pi_{12}^\sim & \Pi_{22} \end{bmatrix}$ where $\Pi_{11} \in \mathbb{RL}_\infty^{m_1 \times m_1}$ and $\Pi_{22} \in \mathbb{RL}_\infty^{m_2 \times m_2}$. Assume $\Pi_{11}(j\omega) > 0$ and $\Pi_{22}(j\omega) < 0$ for all $\omega \in \mathbb{R} \cup \{\infty\}$. Then Π has a J_{m_1,m_2}-spectral factorization.

Proof. The sign definite conditions on Π_{11} and Π_{22} can be used to show that Π has no equalizing vectors (as defined in [27]) and hence the corresponding ARE has a unique stabilizing solution (Theorem 2.4 in [27]). Details are given in [40]. $\qquad\square$